

Synergistic effect of copper nanocrystals-nanoparticles incorporated in a porous organic polymer for the Ullmann C–O coupling reaction

Forough Gorginpour, Hassan Zali-Boeini *

Department of Chemistry, University of Isfahan, 81746-73441, Isfahan, Iran

ARTICLE INFO

Keywords:

Heterogeneous catalysis
Mesoporous materials
Copper nanoparticles
Ullmann C–O coupling

ABSTRACT

A quinoxaline-based porous organic polymer (Q-POP) as a mesoporous organic copolymer was developed as a new platform for the immobilization of CuNPs and copper nanocrystals. The prepared materials were characterized by FT-IR, XRD, N₂ adsorption-desorption isotherms, ICP, TGA, SEM, HR-TEM, EDX, and single-crystal X-ray crystallography. The obtained catalyst presented extraordinary catalytic activity towards Ullmann C–O coupling reactions with high surface area, hierarchical porosity, and excellent thermal and chemical stability. Due to its high porosity, and synergistic effect of copper nanocrystals incorporated in the polymer composite, the as-synthesized catalyst was successfully utilized for the Ullmann C–O coupling reaction of phenols and different aryl halides to prepare various diaryl ether derivatives. All types of aryl halides (except aryl fluorides) were screened in the Ullmann C–O coupling reaction with phenols to produce diaryl ethers in good to excellent yields (70–97 %), and it was found that aryl iodides have the best results. Besides, due to the strong interactions between CuNPs, N, and O-atoms of quinoxaline moiety existing in the polymeric framework, the copper leaching from the support was not observed. Furthermore, the catalyst was recycled and reused for five consecutive runs without significant activity loss.

1. Introduction

In recent years, porous materials have attracted enormous attention in different areas such as catalysis, energy storage, separation, sensing, drug delivery, and so on [1–3]. To date, metal-organic frameworks (MOFs) and covalent organic frameworks (COFs), as porous materials, have been also employed in the various fields [4–12]. However, the reversible nature of chemical bonds in their structure leads to the low thermal and chemical stability under the harsh reaction conditions that restrict their real utilization [13]. In this regard, porous organic polymers (POPs) are an excellent class of porous materials because of their permanent porosity, large surface area, and strong irreversible covalent bonds in the network that result in their superior physical-chemical stability, make them appropriate for the potential applications in the various fields of science [14–24]. Therefore, the design and synthesis of porous organic polymers with organic functional groups in the framework have drawn remarkable research endeavors. For this mean, several synthetic strategies have been developed for the fabrication of POPs [25–32], but most of polymerization methodologies, suffer from expensive noble-metal catalysts, and high temperature. Alternatively,

free radical polymerization of organic monomers with double bonds has been used as a cost-effective, and metal-free strategy for the synthesis of POPs. A nanoporous polydivinylbenzene was prepared via free radical polymerization of divinylbenzene under solvothermal conditions and used as an adsorbent for removing the pollutants from water [33,34]. Using pre-functionalized strategies, a variety of functionalized porous organic polymers have been acquired via free radical co-polymerization of functional monomers containing double bonds and divinylbenzene and demonstrated wide applications in various areas [35–40].

Ullmann cross-coupling for carbon-heteroatom bonds formation is one of the most powerful and convenient approaches for the synthesis of valuable compounds with rich applications in the areas of pharmaceutical, biological, and material chemistry [41–49]. The homogeneous copper-catalyzed Ullmann coupling in the presence of diverse ligand is one of the conventional methods for carbon-heteroatom bonds formation [50–55]. However, these homogeneous Cu-catalyzed coupling systems suffer from the difficulties including separation from the products, non-reusability, and the use of expensive ligands, which limit their wide usage. By consideration of all of the abovementioned drawbacks of homogeneous catalysis, remarkable attention has been focused on

* Corresponding author.

E-mail address: h.zali@chem.ui.ac.ir (H. Zali-Boeini).

<https://doi.org/10.1016/j.mcat.2021.111460>

Received 16 November 2020; Received in revised form 3 February 2021; Accepted 4 February 2021

Available online 15 February 2021

2468-8231/© 2021 Elsevier B.V. All rights reserved.

developing the heterogeneous catalysis due to simplicity of workup, reusability, and minimization of metal contamination of products [56–61]. Recently, the porous organic polymers (POPs) have been utilized as promising host and support to immobilize active catalytic metal species due to their unique properties [62–64]. For instance, Xiao et al. [65] reported incorporation of copper cations into Schiff-based modified PDVB that indicated excellent performance for Ullmann biaryl ether coupling reaction. Mondal et al. [66] successfully deposited Cu nanoparticles on nanoporous polymer DVAC-1 and found that Cu⁰ supported on nanoporous polymer showed extraordinary catalytic activity for Ullmann coupling of aryl halides and amines in water.

In this contribution, we describe the preparation of a quinoxaline-based porous organic polymer (Q-POP) as a new functionalized mesoporous organic polymer with extraordinary porosity and high stability for immobilization of Cu⁰ nanoparticles (CuNPs) and the preparation of CuNPs@Q-POP catalyst (Scheme 1). This novel heterogeneous catalyst demonstrated superior catalytic activity and recyclability for C–O coupling reactions of phenols with aryl halides.

2. Experimental section

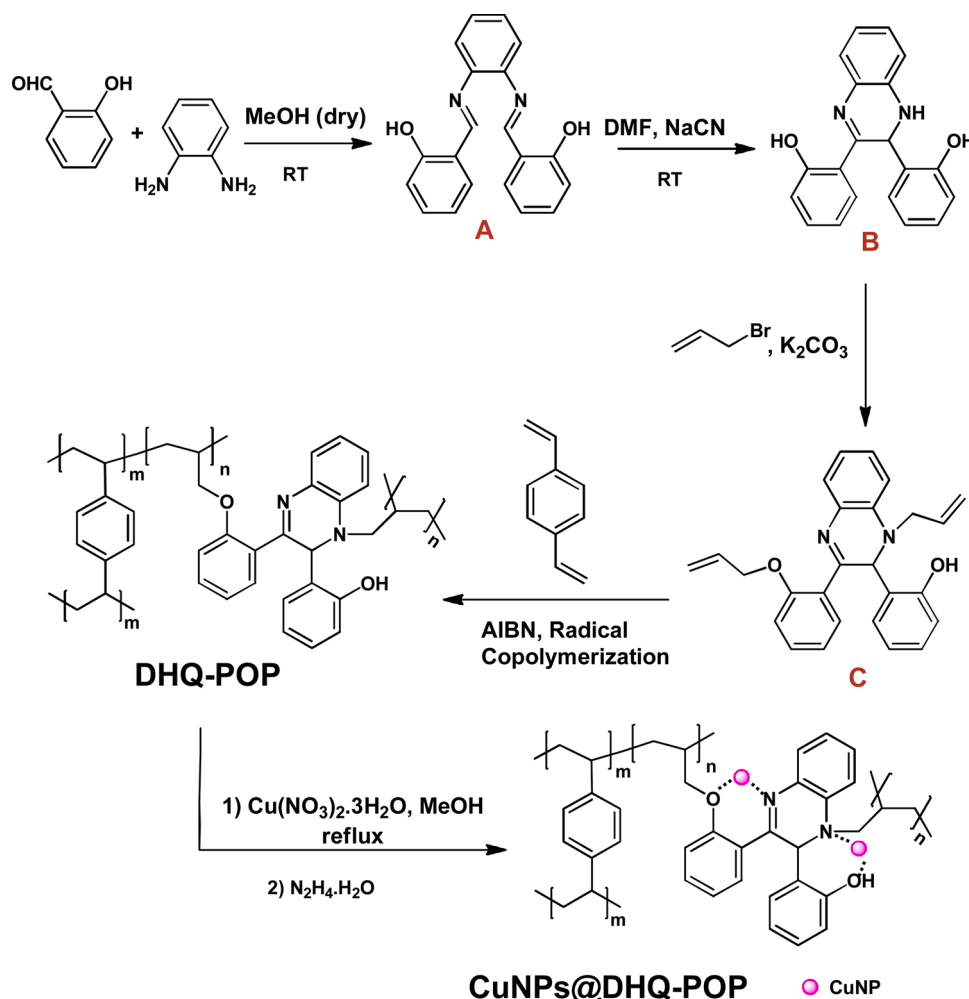
2.1. Materials and instruments

All chemicals were purchased from commercial sources and used without further purification. Solvents used in this study were dried and purified using standard procedures before usage. The powder X-ray diffraction (XRD) patterns of samples were performed on a D8 Advance

Bruker X-ray diffractometer using Cu K α ($\lambda = 1.54^\circ\text{A}$) radiation. Nitrogen sorption isotherms were carried out using a BELsorb-mini 2 at 77 K. The specific surface areas and the pore size distributions of materials were determined by the Brunauer-Emmett-Teller (BET) method and the Barrett-Joyner-Halenda (BJH) model, respectively. Before analysis, the samples were outgassed at 120 °C for 4 h under vacuum. The Fourier transform infrared (FT-IR) spectra were recorded on Jasco FTIR-6300 spectrometer as KBr pellets. Thermal gravimetric analysis (TGA) was obtained using an SDT Q600 instrument by heating samples from 25 to 600 °C in a dynamic argon atmosphere with a heating rate of 10 °C min⁻¹. Field-emission scanning electron (FE-SEM) microscopy and energy-dispersive X-ray spectroscopy (EDX) analysis were carried out on a Tescan Mira3 scanning electron microscope. Transmission electron microscopy (TEM) images were performed on Philips-CM120. Inductively coupled plasma (ICP) was measured on an Analytic Jena PQ9000 for the determination of Cu content. ¹H NMR (400 MHz) and ¹³C NMR (100 MHz) spectra were recorded on a Bruker Avance 400 MHz NMR spectrometer.

2.2. Synthesis of bis(salicylidene)-O-phenylene diamine (A)

This compound was prepared according to the procedure reported in the literature [67]. A solution of o-phenylenediamine (2.16 g, 20 mmol) in dry methanol (30 mL) was added to a solution of salicylaldehyde (4.24 mL, 40 mmol) in dry methanol (20 mL) at room temperature. After stirring for 16 h, the resulting solid was separated by filtration. The obtained solid was washed with methanol and dried *in vacuo* to afford



Scheme 1. Synthetic strategy for fabrication of Q-POP and CuNPs@Q-POP.

compound (A) as yellow powders (6 g, 95 %).

2.3. Synthesis of 2,3-di(2-hydroxyphenyl)1,2-dihydro quinoxaline (B)

Under an argon atmosphere, NaCN (0.226 g, 4.6 mmol) was introduced into a solution of bis(salicylidene)-o-phenylenediamine (3.7 g, 11.8 mmol) in dry DMF (35 mL), and the mixture was stirred at room temperature for 48 h. Subsequently, the reaction mixture was poured into ice water (50 mL). The resultant solid was filtered *via* Buchner funnel, washed with water for several times, and dried. The crude product was purified by recrystallization in acetonitrile. Finally, the pure desired product was obtained as an orange solid (2.96 g, 80 %). ¹H-NMR (400 MHz, CDCl₃): δ 14.92 (s, 1 H), 10.18 (s, 1 H), 7.44 (d, *J* = 8 Hz, 1 H), 7.33–7.29 (m, 1 H), 7.24 (d, *J* = 8 Hz, 1 H), 7.08–7.04 (m, 1 H), 7.01–6.96 (m, 1 H), 6.92–6.86 (m, 4 H), 6.81–6.77 (m, 1 H), 6.66 (s, 1 H), 6.64 (s, 1 H), 6.62–6.59 (m, 1 H), 6.225 (d, *J* = 4 Hz, 1 H); ¹³C-NMR (100 MHz, CDCl₃): δ 161.7, 161.1, 152.6, 136.8, 132.6, 129.3, 129.1, 128.9, 127.4, 127.0, 125.7, 119.4, 118.5, 117.5, 117.2, 117.1, 115.7, 114.1, 45.5.

2.4. Synthesis of allyl-functionalized 2,3-di(2-hydroxy phenyl)1,2-dihydroquinoxaline (C)

A solution of 2,3-di(2-hydroxyphenyl)1,2-dihydro quinoxaline (2.96 g, 9.4 mmol) in acetone (60 mL) was shaken with K₂CO₃ (3.9 g, 28.2 mmol). Allyl bromide (2.44 mL, 28.2 mmol) was then added slowly to the solution. After the mixture was stirred at room temperature for 48 h, water was added (20 mL) and the product was extracted with ethyl acetate (3 × 30 mL) and dried over MgSO₄. The solvent was evaporated under vacuum and the crude product was purified by column chromatography on silica gel (EtOAc/hexane 1:4) to yield allyl functionalized 2,3-di(2-hydroxyphenyl)1,2-dihydroquinoxaline monomer as an orange powder (1.86 g, 50 %). ¹H-NMR (400 MHz, CDCl₃): δ 14.98 (s, 1 H), 7.31 (d, *J* = 8 Hz, 1 H), 7.29 (d, *J* = 8 Hz, 1 H), 7.17–7.02 (m, 4 H), 6.88 (d, *J* = 8 Hz, 1 H), 6.79 (d, *J* = 8 Hz, 1 H), 6.71–6.64 (m, 3 H), 6.55 (d, *J* = 8 Hz, 1 H), 6.30 (s, 1 H), 6.14–6.07 (m, 1 H), 5.61–5.54 (m, 1 H), 5.46 (dd, *J* = 18 Hz, *J* = 4 Hz, 1 H), 5.32 (dd, *J* = 10 Hz, *J* = 4 Hz, 1 H), 5.03 (dd, *J* = 18 Hz, *J* = 4 Hz, 1 H), 4.97 (dd, *J* = 12 Hz, *J* = 4 Hz, 1 H), 4.63–4.62 (m, 2 H), 3.92–3.91 (m, 2 H). ¹³C-NMR (100 MHz, CDCl₃): δ 161.5, 160.0, 152.3, 135.8, 132.6, 131.9, 131.3, 129.9, 128.9, 128.1, 127.9, 126.4, 126.3, 125.5, 120.8, 117.2, 116.9, 116.6, 116.5, 115.5, 111.3, 110.5, 68.0, 50.6, 50.5.

2.5. Synthesis of Q-POP

Radical copolymerization of ligand C with divinylbenzene (DVB) as cross-linker, in the presence of azobisisobutyronitrile (AIBN) as a radical initiator, was used to synthesis the nanoporous polymer under solvothermal conditions. Typically, the monomer C (1 g, 2.52 mmol) and divinylbenzene (1.43 mL, 10.1 mmol) were dissolved in dry DMF (10 mL), followed by the addition of AIBN (0.05 g). The reaction mixture was degassed with argon gas for 30 min, transferred into a 50 mL stainless steel autoclave, and heated at 100 °C for 24 h. After cooling to room temperature, water (30 mL) was added to the reaction mixture and the resulting polymer was filtered and washed with excess water. Additionally, the as-prepared polymer was further washed with methanol for the elimination of any unreacted monomer C. Finally, the desired polymer was obtained as a yellow powder and dried in an oven at 90–100 °C overnight.

2.6. Synthesis of CuNPs@Q-POP(7.3 % Cu)

To a round-bottom flask were introduced Q-POP (1.5 g), MeOH (50 mL), and Et₃N (1 mL). The resultant suspension was allowed to stir at room temperature for 1 h. Then, Cu(NO₃)₂·3H₂O (0.8 g) in MeOH (20 mL) was added to the above suspension and refluxed for about 12 h. The

green Cu²⁺@Q-POP was isolated by filtration, washed with MeOH for removal of excess Cu(NO₃)₂·3H₂O, and then dried *in vacuo* for overnight. Next, CuNPs@Q-POP was synthesized by the reduction of Cu²⁺@Q-POP. An aqueous solution of hydrazine hydrate (10 mL, 35 %) was added dropwise with vigorous stirring under argon atmosphere to a mixture of Cu²⁺@Q-POP (1.5 g), EtOH (17.5 mL), H₂O (10 mL), and NH₄OH (17.5 mL, 25 %). Afterward, the mixture was transferred into a 100 mL stainless steel autoclave and treated at 100 °C for 4 h. Finally, the mixture was filtered and washed with water and methanol successively. The resultant brown solid was dried under vacuum to obtain CuNPs@Q-POP. Inductively coupled plasma (ICP) analysis displayed a Cu content of 7.3 % in the CuNPs@Q-POP.

2.7. Synthesis of CuNPs@Q-POP(2.8 % Cu)

To a round-bottom flask, Q-POP (1.5 g) was suspended in a mixture of MeOH (50 mL) and Et₃N (1 mL). The resultant suspension was allowed to stir at room temperature for 1 h. Then, Cu(NO₃)₂·3H₂O (0.2 g) in MeOH (6 mL) was added and refluxed for about 12 h and the resultant green Cu²⁺@Q-POP precipitate was filtered, washed with MeOH, and dried *in vacuo* overnight. Next, an aqueous solution of hydrazine hydrate (5 mL, 35 %) was added dropwise with intense stirring under argon atmosphere to the mixture of Cu²⁺@Q-POP (1.5 g), EtOH (17.5 mL), H₂O (10 mL), and NH₄OH (17.5 mL, 25 %). Then, the mixture was heated at 100 °C for 4 h in an appropriate stainless steel autoclave. Finally, the mixture was filtered and successively washed with water and methanol. Thereafter, the brown solid was dried under vacuum to obtain CuNPs@Q-POP. Inductively coupled plasma (ICP) analysis revealed that the Cu content of CuNPs@Q-POP was 2.8 %.

2.8. General procedure for O-arylation of phenol with aryl halides catalyzed by CuNPs@Q-POP(7.3 % Cu)

In a typical reaction in a 25 mL round bottom flask (two necked-flask) a mixture of aryl halide (1 mmol), phenol (1.2 mmol), K₂CO₃ (2 mmol), DMF (2 mL) and CuNPs@Q-POP(7.3 % Cu) catalyst (75 mg) was stirred under nitrogen atmosphere at 110 °C for 24. After the reaction, ethyl acetate (10 mL) was added to the reaction mixture and the catalyst was separated by filtration and washed with ethyl acetate. After water (10 mL) was added to the filtrate, extracted with ethyl acetate (2 × 10 mL) and the organic phase was dried with anhydrous MgSO₄. The organic phase was analyzed by GC to determine conversion and selectivity. Then the solvent was removed under reduced pressure and the crude product was purified by column chromatography over silica gel to obtain the desired product. The product was analyzed by ¹H-NMR and ¹³C-NMR.

3. Results and discussion

3.1. Synthesis of Q-POP mesoporous polymer and CuNPs@Q-POP catalyst

Scheme 1 represents the synthetic pathway of Q-POP and CuNPs@Q-POP. Initially, the bis(salicylidene)-o-phenylenediamine (salophen) A was prepared through the reaction of O-phenylenediamine with salicylaldehyde.

Then, 2,3-di(2-hydroxyphenyl)1,2-dihydroquinoxaline B was obtained *via* cyanide-catalyzed cyclization reaction of the salophen under the argon atmosphere. After that, allylation of B with allyl bromide produced diallyl derivative of 2,3-di(2-hydroxyphenyl)1,2-dihydro quinoxaline C monomer as a new ligand. Subsequently, the desired Q-POP was synthesized by the free-radical copolymerization of ligand C and divinylbenzene (DVB) as the cross-linker, using azobisisobutyronitrile (AIBN) as the radical initiator under solvothermal conditions in the form of yellow solid.

The resultant polymer was insoluble in water and common organic

solvents such as MeOH, THF, acetone, acetonitrile, DMF, and DMSO. Finally, after the treatment of Q-POP with a solution of $\text{Cu}(\text{NO}_3)_2 \cdot 3\text{H}_2\text{O}$ in methanol, Cu^{2+} @Q-POP was yielded as a green solid. Indeed, Cu^{2+} ions were immobilized on Q-POP through strong coordination bonds with N and O-atoms present in Q-POP. In the end, CuNPs@Q-POP catalyst was produced as a deep brown solid through reduction reaction of Cu^{2+} ions to CuNPs using hydrazine hydrate as the reducing agent. The copper content in the CuNPs@Q-POP was determined by inductively coupled plasma (ICP) analysis.

3.2. Characterization of DHQ ligand, Q-POP polymer, and CuNPs@Q-POP catalyst

The formation of compound **B** as the key structure of the CuNPs@Q-POP was evidenced by its ^1H and ^{13}C NMR spectra and finally confirmed by its X-ray single crystallography analysis (SCXRD, CCDC 1953774, Fig. 1).

Fourier transform infrared spectroscopy (FT-IR) was applied to confirm the incorporation of ligand C in the polymeric network (Fig. 2a). The appearance of extra new bands at 1167.6 cm^{-1} and 1061.6 cm^{-1} assigned to the CN and CO— stretching vibrations emerged in the Q-POP structure compared with the FT-IR spectra of PDVB, implies that ligand C was successfully copolymerized with divinylbenzene.

The wide-angle X-ray diffraction (WAXRD) pattern of Q-POP and CuNPs@Q-POP are demonstrated in Fig. 2b. The Q-POP illustrates only one broad diffraction peak, indicating that the as-synthesized polymer possesses an amorphous framework. On the other hand, the XRD pattern of CuNPs@Q-POP displays three additional diffraction peaks at $2\theta = 43.45^\circ$, 50.5° , and 74.6° related to diffractions of the (111), (200), (220) planes, along with one broad peak as compared with Q-POP XRD pattern. These observations validated the existence of CuNPs in CuNPs@Q-POP.

Thermal stabilities of Q-POP and CuNPs@Q-POP were determined by thermal gravimetric analysis (TGA) under argon atmosphere. Fig. 2c displays that both of these compounds have excellent thermal stabilities up to 300°C , which could be attributed to the existence of a cross-linked network.

The porosity of Q-POP and CuNPs@Q-POP were measured by nitrogen adsorption and desorption isotherms at 77 K (Fig. 3a). The isotherms for both Q-POP and CuNPs@Q-POP illustrate a slight nitrogen

uptake at low relative pressure and a steep uptake with a vivid hysteresis loop at a high relative pressure (P/P_0) of above 0.6, implying type-IV plus type-I isotherm behavior. Therefore, according to the hysteresis loop present in N_2 sorption isotherm and the distribution curves of the pore size using the BJH model (Fig. 3b), both compounds possess hierarchical porosity structure with dominant mesopores, which is highly desirable for promoting the mass transfer of reactants and better catalytic activity.

The BET surface area of Q-POP and CuNPs@Q-POP were 632.1 and $555.9\text{ m}^2\text{ g}^{-1}$, respectively (Table 1).

Fig. 4 displays the scanning electron microscopy (SEM) images of Q-POP and CuNPs@Q-POP. Q-POP shows a spherical morphology with spheres involving tiny irregular particles interconnected with each other. In addition, agglomerated particles and abundant nanoporosity can be seen in the SEM image (Fig. 4a and b). It should be mentioned that SEM images of CuNPs@Q-POP are approximately similar to Q-POP, indicating that morphology is well preserved after Cu loading (Fig. 4c and d).

To evidence the presence of C, O, N and Cu elements in the CuNPs@Q-POP, the elemental mapping and energy-dispersive X-ray spectroscopy (EDX) were carried out (Fig. 4e-h). The elemental mapping images indicate that Cu nanoparticles are rather uniformly dispersed in the porous organic polymer.

The high-resolution transmission electron microscopy (HR-TEM) is shown in Fig. 4i. As revealed in TEM image CuNPs@Q-POP are composed of polymeric frameworks in which the CuNPs are consistently distributed on the Q-POP without the obvious agglomeration. Additionally, the TEM image demonstrates that copper nanocrystals were distributed between the polymeric networks to form a composite.

3.3. O-arylation of phenol with aryl halides catalyzed by CuNPs@Q-POP

The catalytic efficiency of CuNPs@Q-POP was examined as an active catalyst for C—O cross-coupling reaction of phenols with aryl halides. At the outset of our study, we selected the reaction of phenol with iodobenzene in PEG-200 at 110°C with CuNPs@Q-POP (7.3 mol% Cu° loading) for the synthesis of diphenyl ether as the model reaction. The reaction proceeded with a little yield within 24 h (Table 2, entry 1). Then, other solvents such as DMF, toluene, and H_2O were screened to obtain the highest conversion (Table 2, entries 2–4). When this reaction was performed in DMF in the presence of CuNPs@Q-POP (7.3 mol% Cu° loading), nearly complete conversion (97 %) was obtained and hence, DMF was chosen as the reaction solvent. To investigate the effect of Cu loading amount of CuNPs@Q-POP in the course of the reaction, the process was carried out with CuNPs@Q-POP (2.8 mol% copper loading). It was found that in this case, the conversion rate for the formation of diphenyl ether was considerably reduced (Table 2, entry 5). Therefore, CuNPs@Q-POP (7.3 mol% Cu° loading) was considered to attain the highest conversion for the C—O coupling reactions. To determine the effect of the amount of catalyst on the cross-coupling reaction of phenol and iodobenzene, the reaction was also performed at various amounts of catalyst. We found that the conversion rate of the reaction was decreased from 97 to 70 and 55 % when the amount of catalyst was reduced from 75 to 50, and to 25 mg respectively (Table 2, entries 6 and 7). Additionally, in the arylation of phenol with iodobenzene, K_2CO_3 was discovered to be the most appropriate base, whereas other bases such as NaOH, K_3PO_4 , and Et_3N were not suitable and offered a conversion rate of 60 %, 70 %, and 10 % for diphenyl ether respectively (Table 2, entries 8–10). The control experiment without Cu loading into Q-POP was accomplished to confirm the role of CuNP in this reaction and unveiled that, no desired product was generated (Table 2, entry 14). Screening of the reaction temperature also revealed that decreasing the temperature from 110°C to 90°C reduces the reaction conversion from 97 to 54 % at the same reaction time (Table 2, entry 15). The reaction at a shorter time (12 h) resulted in lower conversion (Table 2, entry 16). In light of all the above mentioned findings, the best conversion and selectivity for the O-

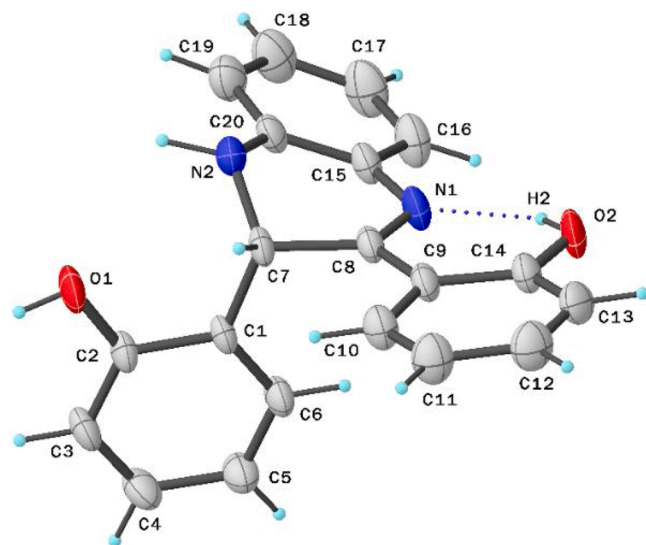


Fig. 1. ORTEP representation of compound **B**. Displacement ellipsoids are drawn at the 30 % probability level and H atoms are shown as small spheres of arbitrary radii. The unit cell contains two independent molecules. Only one molecule is showed for clarity.

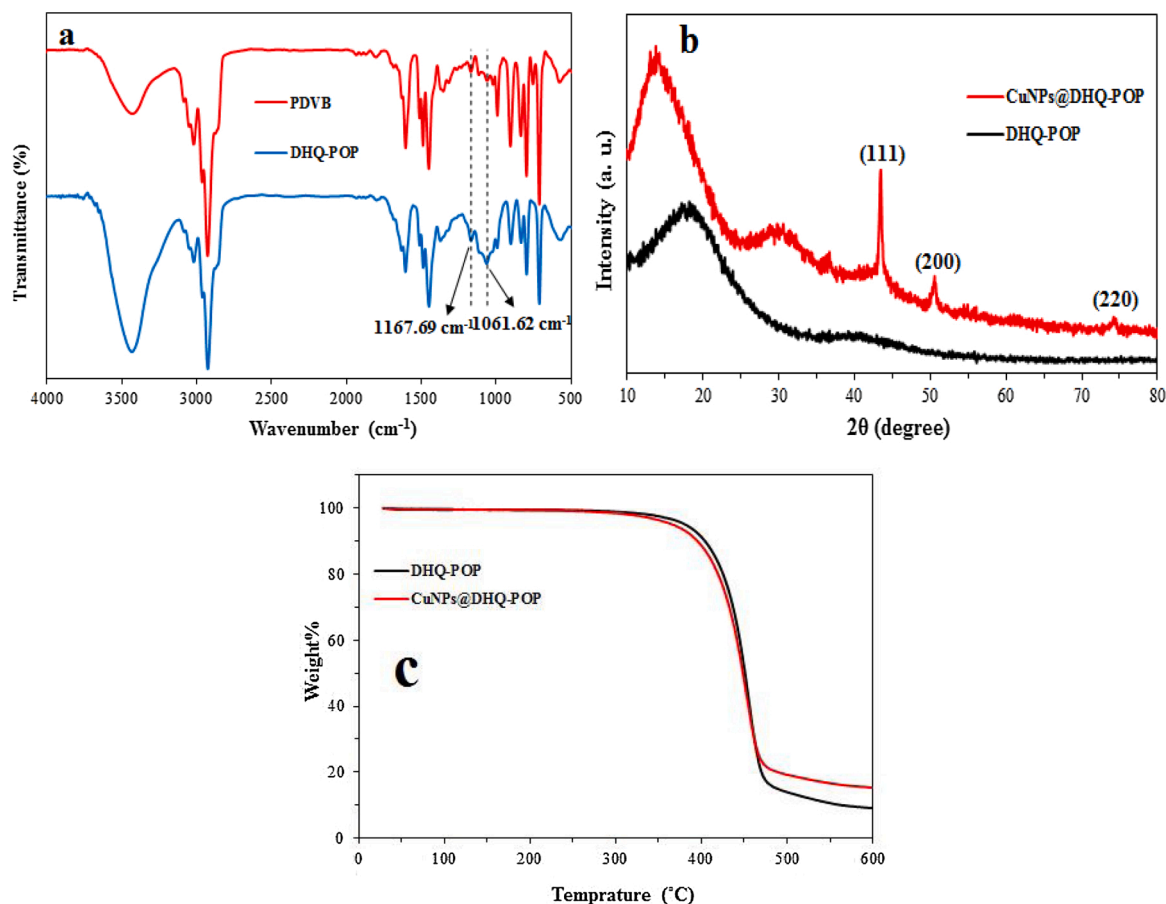


Fig. 2. (a) FT-IR spectra of PDVB and Q-POP; (b) Wide-angle powder XRD patterns of Q-POP and CuNPs@Q-POP; (c) TGA curves of Q-POP and CuNPs@Q-POP.

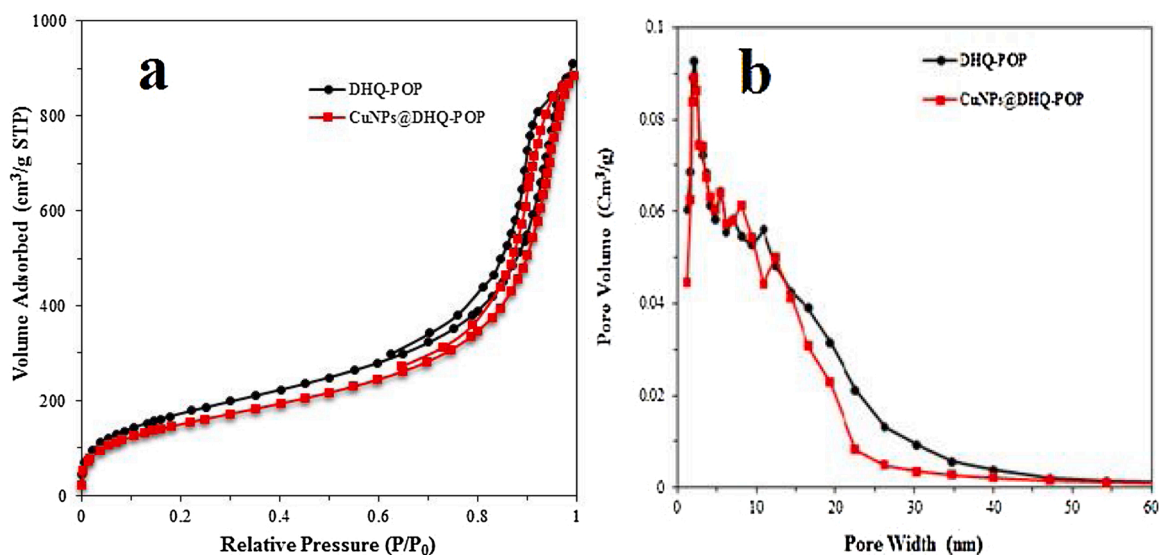


Fig. 3. (a) N₂ sorption isotherms of Q-POP and CuNPs@Q-POP at 77 K; (b) Pore size distribution of Q-POP and CuNPs@Q-POP calculated by BJH model.

Table 1
Textural Parameters for Q-POP and CuNPs@Q-POP.

Material	S _{BET} (m ² /g)	V _P (cm ³ /g)	D _P (nm)
Q-POP	632.1	1.40	8.9
CuNPs@Q-POP	555.9	1.36	9.8

arylation of iodobenzene with phenol was obtained using K₂CO₃ as the base, DMF as the solvent, and in presence of 75 mg of CuNPs@Q-POP (7.3 mol% Cu⁺ loading) at 110 °C for 24 h.

Afterward, with the optimum conditions in hand, the scope of the C—O coupling reaction of phenols with iodobenzene was extended using several types of substituted phenols in presence of CuNPs@Q-POP, and the results are exhibited in Table 3. *Para*-substituted phenols containing

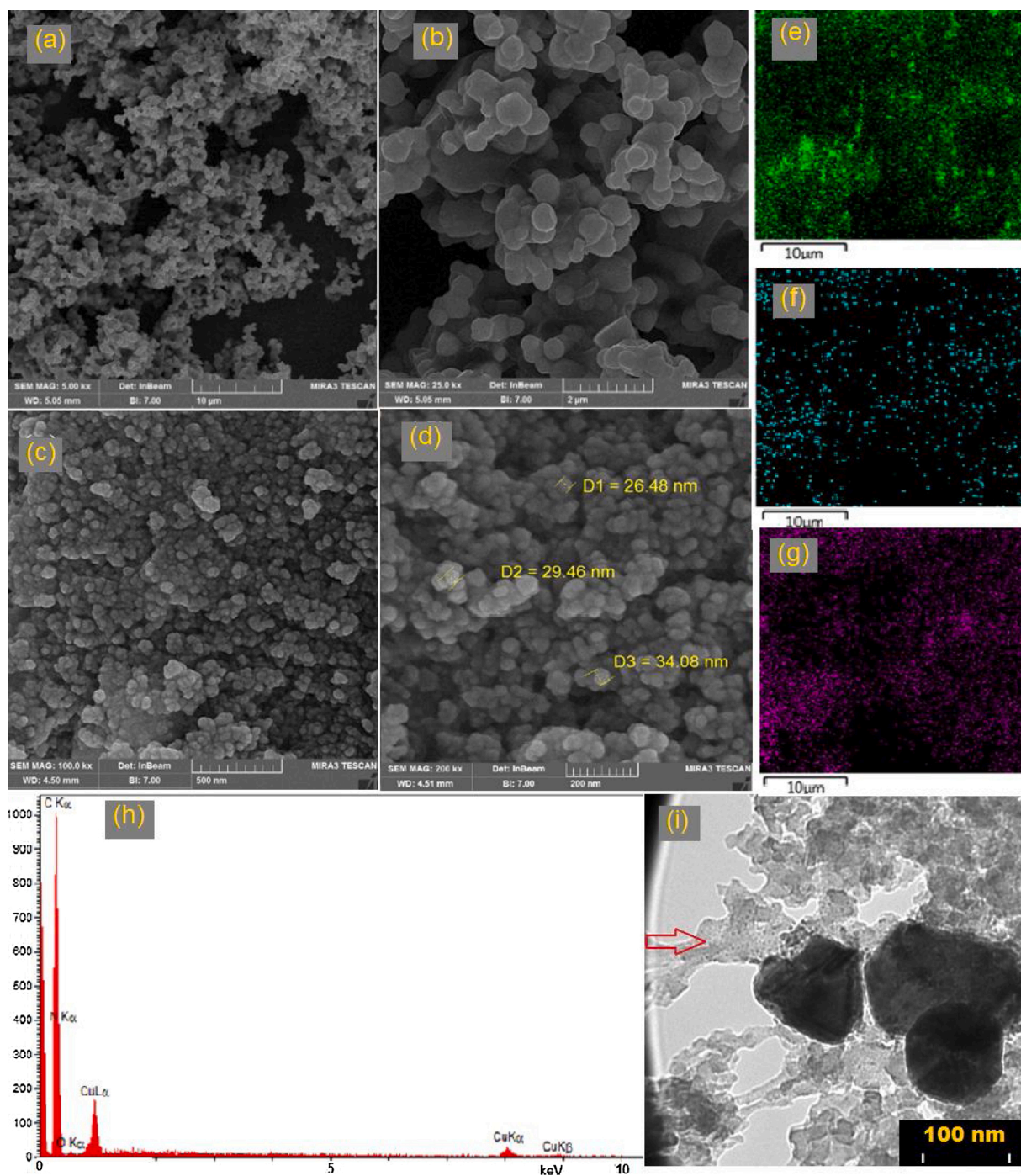


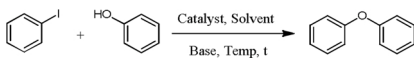
Fig. 4. SEM images of (a and b) Q-POP and (c and d) CuNPs@Q-POP, (e) Cu, (f) N, and (g) O elemental mapping of CuNPs@Q-POP, (h) EDX spectrum of Cu, N, and O, and (i) HR-TEM image of CuNPs@Q-POP.

electron donating such as $-Me$, $-OMe$, and $-t-Bu$ were completely converted to the corresponding diaryl ethers with exceptional selectivity (Table 3, entries 2–4). The conversion for phenols bearing electron-withdrawing substituents such as 3- NO_2 , 4- Cl , and 4- CHO was lower than electron-donating phenols but the selectivity of products was again 100 % (Table 3, entries 5–7). 1-naphthol and 2-naphthol also demonstrated excellent conversions (92 and 94 % respectively) with 100 % selectivity of the desired ethers under the optimized conditions (Table 3, entries 8 and 9). Similarly, 8-hydroxyquinoline was converted into an *O*-arylated product with excellent conversion rate and the selectivity (Table 3, entry 10). Besides, 2,7-dihydroxynaphthalene generated mono aryl ether product with 92 % conversion and 80 % selectivity while the

stoichiometric ratio of iodobenzene: 2,7-dihydroxynaphthalene was 1:1 (Table 3, entry 11). Interestingly, when the same reaction was conducted at iodobenzene to the 2,7-dihydroxynaphthalene ratio (3:1) at prolonged reaction time (48 h), the bis-arylated product was produced with 88 % conversion and 75 % selectivity (Table 3, entry 12). This distinct trend for large molecules was probably ascribed to the high surface area and hierarchical porosity present in the catalyst that facilitates the diffusion of bulky reactant molecules into the pores and increases the chance of reactants to have efficient collision and interaction with catalytic active centers. Furthermore, the reaction with bromobenzene instead of iodobenzene led to the formation of diphenyl ether with 80 % conversion and 100 % selectivity (Table 3, entry 13), while

Table 2

Optimization of various parameters on the cross coupling of iodobenzene and phenol^a.

						
Entry	Catalyst	Cat. (mg)	Solv.	Base (mmol)	Con. (%) ^b	Sel. (%) ^b
1	CuNPs@Q-POP (7.3 %)	75	PEG-200	K ₂ CO ₃ (2)	25	100
2	CuNPs@Q-POP (7.3 %)	75	DMF	K ₂ CO ₃ (2)	97	100
3	CuNPs@Q-POP (7.3 %)	75	Tolu.	K ₂ CO ₃ (2)	<10	–
4 ^c	CuNPs@Q-POP (7.3 %)	75	H ₂ O	K ₂ CO ₃ (2)	0	–
5	CuNPs@Q-POP (2.8 %)	75	DMF	K ₂ CO ₃ (2)	55	100
6	CuNPs@Q-POP (7.3 %)	50	DMF	K ₂ CO ₃ (2)	70	100
7	CuNPs@Q-POP (7.3 %)	25	DMF	K ₂ CO ₃ (2)	55	100
8	CuNPs@Q-POP (7.3 %)	75	DMF	NaOH (2)	60	100
9	CuNPs@Q-POP (7.3 %)	75	DMF	K ₃ PO ₄ (2)	70	100
10	CuNPs@Q-POP (7.3 %)	75	DMF	Et ₃ N (2)	10	100
11	CuNPs@Q-POP (7.3 %)	75	DMF	K ₂ CO ₃ (1.5)	83	100
12	CuNPs@Q-POP (7.3 %)	75	DMF	K ₂ CO ₃ (0.5)	45	100
13	CuNPs@Q-POP (7.3 %)	75	DMF	–	trace	–
14	Q-POP	75	DMF	K ₂ CO ₃ (2)	0	–
15 ^d	CuNPs@Q-POP (7.3 %)	75	DMF	K ₂ CO ₃ (2)	54	100
16 ^e	CuNPs@Q-POP (7.3 %)	75	DMF	K ₂ CO ₃ (2)	70	100

^a Reaction condition: iodobenzene (1 mmol), phenol (1.2 mmol), catalyst, solvent (2.5 mL), base (2 mmol), 110 °C, 24 h. ^b Conversion and selectivity were determined by GC. ^c The reaction was performed in an autoclave. ^d 90 °C. ^e 12 h.

very little amount of diphenyl ether was detected (<10 %) when chlorobenzene was used (Table 3, entry 14).

3.4. The Comparison of our method with some reported method in the literature

In Table 4, the catalytic performance of CuNPs@Q-POP in the O-arylation of iodobenzene with phenol are compared with other reported heterogeneous catalysts [63,65,68–70]. Compared to other catalysts, our synthesized CuNPs@Q-POP catalyst demonstrates better or comparable performance. It can be probably attributed to the synergistic effects of high surface area and the hierarchical porosity together with the superior stability, which enhance diffusion of reactants inside the polymeric network and efficient access to catalytic sites.

To check the recyclability of the catalyst, CuNPs@Q-POP as a solid was separated from the reaction mixture by filtration and then washed with water, ethyl acetate, and methanol, respectively, and dried under vacuum. Ultimately, the isolated and refined catalyst was applied for numerous consecutive recycle runs under the optimized reaction conditions. It was found that the recycled catalyst, for the C–O cross-coupling reaction could be reused five times without appreciable reduction in the conversion rate and selectivity (Fig. 5a). Wide-angle X-ray diffraction (WAXRD) patterns of the reused CuNPs@Q-POP after the fifth run were similar to the fresh nanocatalyst (Fig. S2). The SEM images indicate that the morphology of CuNPs@Q-POP is well maintained after five runs (Fig. S3). A hot filtration test was further accomplished to remove CuNPs@Q-POP and survey the heterogeneous nature of

Table 3

Ullmann O-arylation reaction catalyzed by CuNPs@Q-POP(7.3 % Cu)^a.

Entry	Aryl halides	Nucleophiles	Products	Conv. (%) ^b	Sel. (%) ^b
1				97	100
2				97	100
3				91	100
4				90	100
5				85	100
6				70	100
7				89	100
8				92	100
9				94	100
10				95	100
11				92	80
12 ^c				77	75
13				80	100
14				<10	–

^a Reaction condition: aryl halide (1 mmol), phenol (1.2 mmol), K₂CO₃ (2 mmol), DMF (2 mL), CuNPs@Q-POP (7.3 % Cu, 75 mg), 110 °C, 24 h, under N₂ atmosphere. ^b Conversion and selectivity were determined by GC. ^c Reaction conditions for the synthesis of bis-arylated product: iodobenzene (3 mmol), 2,7-dihydroxynaphthalene (1 mmol), K₂CO₃ (4 mmol), DMF (4 mL), CuNPs@Q-POP (7.3 % Cu, 150 mg), 110 °C, 48 h, under N₂ atmosphere.

Table 4

Comparison of catalytic performance of CuNPs@Q-POP catalyst in the O-arylation with the other reported Cu-based catalysts.

Catalyst	Condition	O-arylation	Ref.
CuNPs@Q-POP	K ₂ CO ₃ , DMF, 110 °C	Conversion (97 %), Selectivity (100 %)	This work
Cu@MCTP-1	CS ₂ CO ₃ , DMF, 130 °C	Yield (94 %)	[63]
PDVB-SB-Cu	CS ₂ CO ₃ , DMSO, 115 °C	Yield (91 %)	[65]
Meso Cu/MnOx	K ₂ CO ₃ , DMF, 140 °C	Conversion (88 %), Selectivity (>99 %)	[68]
PS-Cu-Furfural	CS ₂ CO ₃ , DMSO, t-Bu ₄ NBr, 120 °C	Yield (96 %)	[69]
Cu ₂ O/graphene	CS ₂ CO ₃ , THF, 150 °C	Yield (96 %)	[70]

separated CuNPs@Q-POP. In the case of the O-arylation of iodobenzene with phenol under optimized conditions, the catalyst was filtered from the reaction mixture after 8 h (48 % conversion). Then, the reaction of the filtrate was further continued at the same reaction conditions for an additional 16 h. No changes in conversion and selectivity were observed after removing the catalyst (Fig. 5b). This fact implies that no Cu species were detectable in the filtrate and the atomic absorption spectroscopy of the filtrate confirm that. This can be attributed to the strong chemical interaction between CuNPs and N and O binding sites in quinoxaline moiety present in the polymeric network, which prevents leaching of CuNPs from the polymeric network.

The feasibility of a multi-gram scale synthesis was also checked for the catalyst. When the C–O coupling reaction of phenol was performed with iodobenzene in a 50 mmol scale, the resulting diphenyl ether was produced with nearly complete (96 %) conversion.

A reaction pathway is proposed for the N-arylation of iodobenzene with aniline catalysed by CuNPs@Q-POP, and shown in Scheme 2 [71,

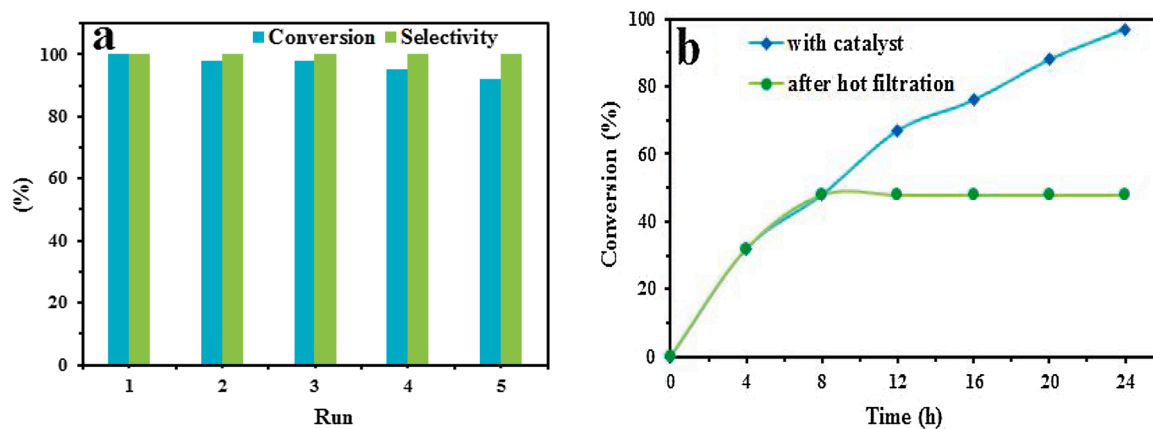
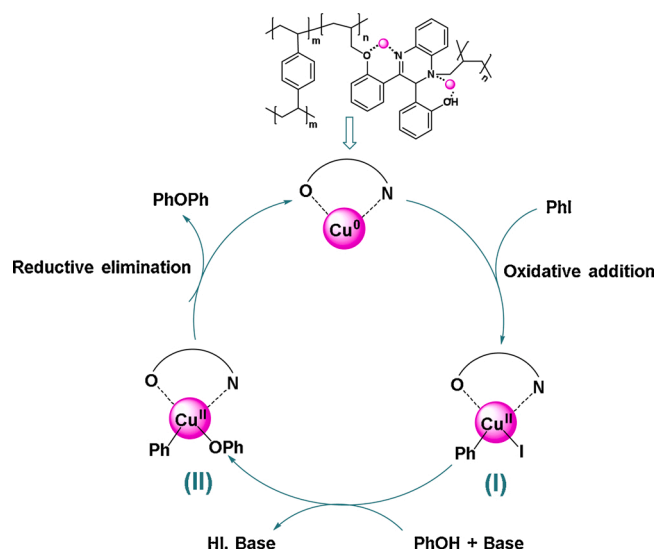


Fig. 5. (a) Recyclability of CuNPs@Q-POP in the Ullmann *O*-arylation reactions, (b) Hot filtration test for CuNPs@DHQ-POP. Reaction conditions for the Cross-Coupling of iodobenzene and phenol: Iodobenzene (1 mmol), phenol (1.2 mmol), K_2CO_3 (2 mmol), DMF (2 mL), CuNPs@Q-POP (7.3 % Cu, 75 mg), 110 °C, 24 h, under N_2 atmosphere.



Scheme 2. A plausible mechanism for the *O*-arylation of iodobenzene with phenol using CuNPs@Q-POP.

72]. At first, an oxidative addition of iodobenzene to Cu^0 nanoparticles occurs, leading to the formation of the intermediate (I). Subsequently, the in-situ produced phenolate ion reacts with the intermediate (I) to give the intermediate (II). Finally, the desired product is obtained by the reductive elimination of intermediate (II).

4. Conclusion

In summary, a robust porous organic polymer (Q-POP), having high surface area, hierarchical porosity was designed and synthesized via a facile metal-free, eco-friendly, and efficient free-radical copolymerization and used for immobilization of copper nanoparticles and nanocrystals to synergistically enhance its catalytic activity in the Ullmann C–O cross-coupling reactions. The extraordinary stability, the hierarchical porosity, as well as open organic pores of the polymeric network allow the CuNPs@Q-POP to provide outstanding catalytic performance in the C–O cross-coupling reaction of aryl halides and phenols. In addition, the presence of N, and O-atoms of quinoxaline moiety within the polymeric framework provide an excellent environment that stabilize CuNPs via strong coordination and/or electrostatic interactions with quinoxaline moiety. Furthermore, the catalyst is easily recoverable and can be reused recycled from the reaction mixture with no vivid loss of

catalytic activity after recycling five times. In one hand we also found that the as-synthesized CuNPs@Q-POP catalyst can be used in other synthetic transformation and on the other hand, Q-POP copolymer has the potential to be used in many other research fields such as the light-emissive layer in OLEDs (due to its intense fluorescence), as adsorbant for the removing of organic chemical pollutants, and toxic heavy metal ions from wastewater.

CRediT authorship contribution statement

Forough Gorginpour: Methodology, Validation, Formal analysis, Investigation, Writing - original draft, Visualization. **Hassan Zali-Boeini:** Supervision, Project administration, Funding acquisition, Writing - review & editing.

Declaration of Competing Interest

The authors report no declarations of interest.

Acknowledgments

The authors are grateful to the University of Isfahan research council for providing instrumental facilities and partial financial support for this work.

Appendix A. Supplementary data

Supplementary material related to this article can be found, in the online version, at doi:<https://doi.org/10.1016/j.mcat.2021.111460>.

References

- [1] M.E. Davis, Ordered porous materials for emerging applications, *Nature* 417 (2002) 813–821.
- [2] A. Thomas, Functional Materials: From Hard to Soft Porous Frameworks, *Angew. Chem. Int. Ed.* 49 (2010) 8328–8344.
- [3] P. Kaur, J.T. Hupp, S.T. Nguyen, Catalysis using multifunctional organosiliceous hybrid materials, *ACS Catal.* 1 (2011) 819–835.
- [4] P. Horcajada, R. Gref, T. Baati, P.K. Allan, G. Maurin, P. Couvreur, G. Férey, R. E. Morris, C. Serre, Metal–Organic frameworks in biomedicine, *Chem. Soc. Rev.* 112 (2012) 1232–1268.
- [5] C.J. Doonan, D.J. Tranchemontagne, T.G. Glover, J.R. Hunt, O.M. Yaghi, Exceptional ammonia uptake by a covalent organic framework, *Nat. Chem.* 2 (2010) 235–238.
- [6] W.-Y. Gao, M. Chrzanowski, S. Ma, Metal–metalloporphyrin frameworks: a resurging class of functional materials, *Chem. Soc. Rev.* 43 (2014) 5841–5866.
- [7] J. Liu, L. Chen, H. Cui, J. Zhang, L. Zhang, C.-Y. Su, Applications of metal–organic frameworks in heterogeneous supramolecular catalysis, *Chem. Soc. Rev.* 43 (2014) 6011–6061.

- [8] Y. Zeng, R. Zou, Y. Zhao, Covalent organic frameworks for CO₂ capture, *Adv. Mater.* 28 (2016) 2855–2873.
- [9] H. Xu, J. Gao, D. Jiang, Stable, crystalline, porous, covalent organic frameworks as a platform for chiral organocatalysts, *Nat. Chem.* 7 (2015) 905–912.
- [10] A.I. Cooper, Conjugated microporous polymers, *Adv. Mater.* 21 (2009) 1291–1295.
- [11] L.E. Kreno, K. Leong, O.K. Farha, M. Allendorf, R.P. VanDuyne, J.T. Hupp, Metal–Organic framework materials as chemical sensors, *Chem. Rev.* 112 (2012) 1105–1125.
- [12] X. Zhu, C. Tian, S. Mahurin, S.-H. Chai, C. Wang, S. Brown, G.M. Veith, H. Luo, H. Liu, S. Dai, A superacid-catalyzed synthesis of porous membranes based on triazine frameworks for CO₂ separation, *J. Am. Chem. Soc.* 134 (2012) 10478–10484.
- [13] J.J. Low, A.I. Benin, P. Jakubczak, J.F. Abrahamian, S.A. Faheem, R.R. Willis, Virtual High, Throughput screening confirmed experimentally: porous coordination polymer hydration, *J. Am. Chem. Soc.* 131 (2009) 15834–15842.
- [14] Y. Zhang, B. Li, S. Ma, Dual functionalization of porous aromatic frameworks as a new platform for heterogeneous cascade catalysis, *Chem. Commun.* 50 (2014) 8507–8510.
- [15] W. Wang, A. Zheng, P. Zhao, C. Xia, F. Li, Au-NHC@Porous organic polymers: synthetic control and its catalytic application in alkyne hydration reactions, *ACS Catal.* 4 (2014) 321–327.
- [16] W. Zhang, B. Aguilu, S. Ma, Potential applications of functional porous organic polymer materials, *J. Mater. Chem. A* 5 (2017) 8795–8824.
- [17] Y. Xu, S. Jin, H. Xu, A. Nagai, D. Jiang, Conjugated microporous polymers: design, synthesis and application, *Chem. Soc. Rev.* 42 (2013) 8012–8031.
- [18] B. Li, Y. Zhang, D. Ma, Z. Shi, S. Ma, Mercury nano-trap for effective and efficient removal of mercury(II) from aqueous solution, *Nat. Commun.* 5 (2014) 5537–5543.
- [19] Y. Zhang, S.N. Riduan, Functional porous organic polymers for heterogeneous catalysis, *Chem. Soc. Rev.* 41 (2012) 2083–2094.
- [20] Y. Zhu, H. Long, W. Zhang, Imine-linked porous polymer frameworks with high small gas (H₂, CO₂, CH₄, C₂H₂) uptake and CO₂/N₂ selectivity, *Chem. Mater.* 25 (2013) 1630–1635.
- [21] Q. Chen, M. Luo, P. Hammershøj, D. Zhou, Y. Han, B.W. Laursen, C.-G. Yan, B.-H. Han, Microporous polycarbazole with high specific surface area for gas storage and separation, *J. Am. Chem. Soc.* 134 (2012) 6084–6087.
- [22] Z. Li, H. Li, H. Xia, X. Ding, X. Luo, X. Liu, Y. Mu, Triarylboron-linked conjugated microporous polymers: sensing and removal of fluoride ions, *Chem. Eur. J.* 21 (2015) 17355–17362.
- [23] Q. Sun, Z. Dai, X. Meng, F.-S. Xiao, Porous polymer catalysts with hierarchical structures, *Chem. Soc. Rev.* 44 (2015) 6018–6034.
- [24] L. Tan, B. Tan, Hypercrosslinked porous polymer materials: design, synthesis, and applications, *Chem. Soc. Rev.* 46 (2017) 3322–3356.
- [25] T. Ben, H. Ren, S. Ma, D. Cao, J. Lan, X. Jing, W. Wang, J. Xu, F. Deng, J. M. Simmons, S. Qiu, G. Zhu, Targeted synthesis of a porous aromatic framework with high stability and exceptionally high surface area, *Angew. Chem. Int. Ed.* 48 (2009) 9457–9460.
- [26] L. Li, H. Zhao, J. Wang, R. Wang, Facile fabrication of ultrafine palladium nanoparticles with size- and location-control in click-based porous organic polymers, *ACS Nano* 8 (2014) 5352–5364.
- [27] B. Li, Z. Guan, W. Wang, X. Yang, J. Hu, B. Tan, T. Li, Highly dispersed Pd catalyst locked in knitting aryl network polymers for suzuki–Miyaura coupling reactions of aryl chlorides in aqueous media, *Adv. Mater.* 24 (2012) 3390–3395.
- [28] B.G. Hauser, O.K. Farha, J. Exley, J.T. Hupp, Thermally enhancing the surface areas of yamamoto-derived porous organic polymers, *Chem. Mater.* 25 (2013) 12–16.
- [29] Y. Zhu, Y. Ji, D. Wang, Y. Zhang, H. Tang, X. Jia, M. Song, G. Yu, G. Kuang, BODIPY-based conjugated porous polymers for highly efficient volatile iodine capture, *J. Mater. Chem. A* 5 (2017) 6622–6629.
- [30] Z.-A. Qiao, S.-H. Chai, K. Nelson, Z. Bi, J. Chen, S.M. Mahurin, X. Zhu, S. Dai, Polymeric molecular sieve membranes via in situ cross-linking of non-porous polymer membrane templates, *Nat. Commun.* 5 (2014) 3705–3712.
- [31] J. Schmidt, J. Weber, J.D. Epping, M. Antonietti, A. Thomas, Microporous conjugated poly(thienylene arylene) networks, *Adv. Mater.* 21 (2009) 702–705.
- [32] L. Chen, Y. Yang, D. Jiang, CMPs as scaffolds for constructing porous catalytic frameworks: a built-in heterogeneous catalyst with high activity and selectivity based on nanoporous metalloporphyrin polymers, *J. Am. Chem. Soc.* 132 (2012) 9138–9143.
- [33] Y. Zhang, S. Wei, F. Liu, Y. Du, S. Liu, Y. Ji, T. Yokoi, T. Tatsumi, F.-S. Xiao, Superhydrophobic nanoporous polymers as efficient adsorbents for organic compounds, *Nano Today* 4 (2009) 135–142.
- [34] Y. Zhang, J.N. Wang, Y. He, Y.Y. He, B.B. Xu, S. Wei, F.-S. Xiao, Solvothermal synthesis of nanoporous polymer chalk for painting superhydrophobic surfaces, *Langmuir* 27 (2011) 12585–12590.
- [35] F. Liu, W. Kong, C. Qi, L. Zhu, F.-S. Xiao, Design and synthesis of mesoporous polymer-based solid acid catalysts with excellent hydrophobicity and extraordinary catalytic activity, *ACS Catal.* 2 (2012) 565–572.
- [36] Z. Guo, X. Cai, J. Xie, X. Wang, Y. Zhou, J. Wang, Hydroxyl-exchanged nanoporous ionic copolymer toward low-temperature cycloaddition of atmospheric carbon dioxide into carbonates, *ACS Appl. Mater. Interfaces* 8 (2016) 12812–12821.
- [37] H. Gao, L. Ding, W. Li, G. Ma, H. Bai, L. Li, Hyper-cross-Linked organic microporous polymers based on alternating copolymerization of Bismaleimide, *ACS Macro Lett.* 5 (2016) 377–381.
- [38] Q. Sun, X. Meng, X. Liu, X. Zhang, Y. Yang, Q. Yang, F.-S. Xiao, Mesoporous cross-linked polymer copolymerized with chiral BINAP ligand coordinated to a ruthenium species as an efficient heterogeneous catalyst for asymmetric hydrogenation, *Chem. Commun. (Camb.)* 48 (2012) 10505–10507.
- [39] Q. Sun, Z. Lv, Y. Du, Q. Wu, L. Wang, L. Zhu, X. Meng, W. Chen, F.-S. Xiao, Recyclable porous polymer-supported copper catalysts for Glaser and huisgen 1,3-diolar cycloaddition reactions, *Chem. Asian J.* 8 (2013) 2822–2827.
- [40] H. Wang, Y. Shi, M. Haruta, J. Huang, Aerobic oxidation of benzyl alcohol in water catalyzed by gold nanoparticles supported on imidazole containing crosslinked polymer, *Appl. Catal. A* 536 (2017) 27–34.
- [41] M. Negwar, Akademik, Berlin. Organic-chemical Drugs and Their Synonyms: (An International Survey), 7th ed., 1994.
- [42] M. Liang, J. Chen, Arylamine organic dyes for dye-sensitized solar cells, *Chem. Soc. Rev.* 42 (2013) 3453–3488.
- [43] F. Monnier, M. Taillefer, Catalytic C–C, C–N, and C–O ullmann-type coupling reactions: copper makes a difference, *Angew. Chem. Int. Ed.* 47 (2008) 3096–3099.
- [44] R.K.V. Devambatla, O.A. Namjoshi, S. Choudhary, E. Hamel, C.V. Shaffer, C. C. Rohena, S.L. Mooberry, A. Gangjee, Design, synthesis, and preclinical evaluation of 4-substituted-5-methyl-furo[2,3-d]pyrimidines as microtubule targeting agents that are effective against multidrug resistant cancer cells, *J. Med. Chem.* 59 (2016) 5752–5765.
- [45] S. Yang, C. Wu, H. Zhou, Y. Yang, Y. Zhao, C. Wang, W. Yang, J. Xu, Synthesis of cyclic peptides constrained with biarylamine linkers using Buchwald–Hartwig C–N coupling, *Adv. Synth. Catal.* 355 (2013) 53–58.
- [46] V. Balraju, J. Iqbal, Synthesis of cyclic peptides constrained with biarylamine linkers using Buchwald–Hartwig C–N coupling, *J. Org. Chem.* 71 (2006) 8954–8956.
- [47] K.C. Nicolaou, C.N.C. Boddy, Atropselective macrocyclization of diaryl ether ring systems: application to the synthesis of vancomycin model systems, *J. Am. Chem. Soc.* 124 (2002) 10451–10455.
- [48] M.Q. Salih, C.M. Beaudry, Enantioselective Ullmann Ether Couplings: syntheses of (–)-Myricatomentogenin, (–)-Juglathanin, (+)-Galeon, and (+)-Pterocarane, *Org. Lett.* 15 (2013) 4540–4543.
- [49] E. Sperotto, G.P.M. van Klink, J.G. de Vries, G. van Koten, Aminoarenethiolato-copper(I) as (pre-)catalyst for the synthesis of diaryl ethers from aryl bromides and sequential C–O/C–S and C–N/C–S cross coupling reactions, *Tetrahedron* 66 (2010) 9009–9020.
- [50] M. Wolter, G. Nordmann, G.E. Job, S.L. Buchwald, Copper-catalyzed coupling of aryl iodides with aliphatic alcohols, *Org. Lett.* 4 (2002) 973–976.
- [51] S. Benyahya, F. Monnier, M.W.C. Man, C. Bied, F. Ouazzani, M. Taillefer, Sol–gel immobilized and reusable copper-catalyst for arylation of phenols from aryl bromides, *Green Chem.* 11 (2009) 1121–1123.
- [52] D. Kundu, S. Bhadra, N. Mukherjee, B. Sreedhar, B.C. Ranu, Heterogeneous Cu^{II}-Catalysed solvent-controlled selective N-Arylation of cyclic amides and amines with bromo-iodoarenes, *Chem. Eur. J.* 19 (2013) 15759–15768.
- [53] A.C. Bissember, R.J. Lundgren, S.E. Creutz, J.C. Peters, G.C. Fu, Transition-metal-catalyzed alkylations of amines with alkyl halides: photoinduced, copper-catalyzed couplings of carbazoles, *Angew. Chem. Int. Ed.* 52 (2013) 5129–5133.
- [54] A. Ouali, J.-F. Spindler, A. Jutand, M. Taillefer, Nitrogen ligands in copper-catalyzed arylation of phenols: Structure/Activity relationships and applications, *Adv. Synth. Catal.* 349 (2007) 1906–1916.
- [55] D. Maiti, S.L. Buchwald, Orthogonal Cu- and Pd-based catalyst systems for the O- and N-Arylation of aminophenols, *J. Am. Chem. Soc.* 131 (2009) 17423–17429.
- [56] B. Sels, D. Devos, M. Buntinx, F. Pierard, A.K. Mesmaeker, P.A. Jacobs, Layered double hydroxides exchanged with tungstate as biomimetic catalysts for mild oxidative bromination, *Nature* 400 (1999) 855–857.
- [57] C. Coperet, M. Chabanas, R.P. Saint-Arroman, J.-M. Basset, Homogeneous and Heterogeneous Catalysis: Bridging the Gap through Surface Organometallic Chemistry, *Angew. Chem. Int. Ed.* 42 (2003) 156–181.
- [58] R.A. Sheldon, Green solvents for sustainable organic synthesis: state of the art, *Green Chem.* 7 (2005) 267–278.
- [59] A. Corma, H. Garcia, Lewis Acids, From conventional homogeneous to green homogeneous and heterogeneous catalysis, *Chem. Rev.* 103 (2003) 4307–4366.
- [60] J.M. Thomas, R. Raja, D.W. Lewis, Single-site heterogeneous catalysts, *Angew. Chem. Int. Ed.* 44 (2005) 6456–6482.
- [61] S. Kramer, F. Hejjo, K.H. Rasmussen, S. Kegnaes, Silylative pinacol coupling catalyzed by nitrogen-doped carbon-encapsulated Nickel/Cobalt nanoparticles: evidence for a silyl radical pathway, *ACS Catal.* 8 (2018) 754–759.
- [62] P. Bhanja, K. Ghosh, S.S. Islam, S.M. Islam, A. Bhaumik, Pd NP-decorated N-rich porous organic polymer as an efficient catalyst for upgradation of biofuels, *ACS Omega* 3 (2018) 7639–7647.
- [63] P. Puthiaraj, W.-S. Ahn, Synthesis of copper nanoparticles supported on a microporous covalent triazine polymer: an efficient and reusable catalyst for O-arylation reaction, *Catal. Sci. Technol.* 6 (2016) 1701–1709.
- [64] J. Yi, H.M. Ahn, J.H. Yoon, C. Kim, S.J. Lee, Preparation of Bispyridine based porous organic polymer as a new platform for Cu(II) catalyst and its use in heterogeneous olefin epoxidation, *New J. Chem.* 42 (2018) 14067–14070.
- [65] L. Wang, J. Zhang, J. Sun, L. Zhu, H. Zhang, F. Liu, D. Zheng, X. Meng, X. Shi, F.-S. Xiao, Copper-incorporated porous polydivinylbenzene as efficient and recyclable heterogeneous catalyst in ullmann biaryl ether coupling, *ChemCatChem* 5 (2013) 1606–1613.
- [66] J. Mondal, A. Biswas, S. Chiba, Y. Zhao, Cu⁰ nanoparticles deposited on nanoporous polymers: a recyclable heterogeneous nanocatalyst for ullmann coupling of aryl halides with amines in water, *Sci. Rep.* 5 (2015) 8294.
- [67] B.J.E. Reich, A.K. Justice, B.T. Beckstead, J.H. Reibenspies, S.A. Miller, Cyanide-catalyzed cyclizations via Aldimine Coupling, *J. Org. Chem.* 69 (2004) 1357–1359.

- [68] K. Mullick, S. Biswas, C. Kim, R. Ramprasad, A.M. Angeles-Boza, S.L. Suib, Ullmann reaction catalyzed by heterogeneous mesoporous Copper/Manganese oxide: a kinetic and mechanistic analysis, *Inorg. Chem.* 56 (2017) 10290–10297.
- [69] Sk.M. Islam, N. Salam, P. Mondal, A.S. Roy, K. Ghosh, K.A. Tuhina, A highly active reusable polymer anchored copper catalyst for C-O, C-N and C-S cross coupling reactions, *J. Mol. Catal. A Chem.* 387 (2014) 7–19.
- [70] Z. Zhai, X. Guo, Z. Jiao, G. Jin, X.-Y. Guo, Graphene-supported Cu₂O nanoparticles: an efficient heterogeneous catalyst for C-O cross-coupling of aryl iodides with phenols, *Catal. Sci. Technol.* 4 (2014) 4196–4199.
- [71] S. Jammi, S. Sakthivel, L. Rout, T. Mukherjee, S. Mandal, R. Mitra, P. Saha, T. Punniyamurthy, CuO nanoparticles catalyzed C-N, C-O, and C-S cross-coupling reactions: scope and mechanism, *J. Org. Chem.* 74 (2009) 1971–1976.
- [72] J. Mondal, A. Modak, A. Dutta, A. Bhaumik, Facile C-S coupling reaction of aryl iodide and thiophenol catalyzed by Cu-grafted furfural functionalized mesoporous organosilica, *Dalton Trans.* 40 (2011) 5228–5235.